Advances in Nano Research, *Vol. 8, No. 3 (2020) 229-244*
DOI: https://doi.org/10.12989/anr.2020.8.3.229

Response of orthotropic Kelvin modeling for single-walled carbon nanotubes: Frequency analysis

Muzamal Hussain*[1], Muhammad N. Naeem [1a] and Abdelouahed Tounsi [2,3]

[1] *Department of Mathematics, Government College University Faisalabad, 38000, Faisalabad, Pakistan*
[2] *Materials and Hydrology Laboratory University of Sidi Bel Abbes, Algeria Faculty of Technology Civil Engineering Department, Algeria*
[3] *Department of Civil and Environmental Engineering, King Fahd University of Petroleum & Minerals, 31261 Dhahran, Eastern Province, Saudi Arabia*

(*Received October 5, 2019, Revised February 14, 2020, Accepted February 24, 2020*)

Abstract. In this paper, modified Kelvin's model has been used to analyze the orthotropic vibration frequencies of single walled carbon nanotubes with clamped-clamped and clamped-free boundary conditions. For this system the governing equation is developed with wave propagation approach. Armchair, zigzag and chiral structures are considered for the vibrational analysis to investigate the effect of different modes, in-plane rigidity and mass density per unit lateral area. Throughout the computations, on decreasing the length-to-diameter ratios, the frequencies of said structure increases. In addition, by increasing three different value of in-plane rigidity resulting frequencies also increase and frequencies decrease on increasing mass density per unit lateral area. The results generated using computer software MATLAB to furnish the evidence regarding applicability of present model and also verified by available published literature.

Keywords: CNTs; wave propagation approach; Kelvin Model; bending rigidity

1. Introduction

CNTs have a variety of applications because of their distinctive molecular structure and show unique electronic and mechanical properties because of their curvature. In addition, they are utilized in different fields such as bioengineering, tissue engineering, computer engineering, optics, energy and environmental systems. Here, a succinct review has been provided regarding different applications of CNTs. Their enormous versatility has made them being coined as a solution looking for problems. Natuski *et al.* (2006) conducted the vibration of nested CNTs in elastic matrix. Flügge shell theory had been engaged to establish administrative shell equations while proposed method was wave propagation. Wang and Liew (2007) studied nano- and micro-tubes using EBM and TBM. The results showed that to indicate the importance of applied theory of beams, the shear effect is evident for the carbon nanotubes. Furthermore, vibrations of nanotubes have been modeled by atomistic/continuum models. actuators, sensors and sonication.

The fundamental frequencies of CNTs have higher values at lower diameter and showed that the chirality have no momentous influence on frequencies of nanotubes. The vacancies are produced due to holes in the graphite structure and due to chemical and theoretical physics, the defects in CNTs reduce the Young's modulus (Kotakoski *et al.* 2006). Usuki and Yogo (2009) formed beam equations again based on Flugge shell theory, they concluded that if nonlocality and refined model are ignored then the generalized beam theory and Flügge theory produce alike results. Owing to this, Gibson *et al.* (2007) presented a coherent review about the simulations, and modeling of vibrating nanotubes. Akgöz and Civalek (2012) examined with the bending analysis of single-walled carbon nanotubes (CNT) based on modified couple stress and strain gradient elasticity theories and Euler–Bernoulli beam theory. The size effect is taken into consideration using the modified couple stress and strain gradient elasticity theories. Kulathunga *et al.* (2009) widely explored the classical shell theory to compute the strain of SWCNTs. It has been calculated for the first time from this formula in the absence of length-diameter ratio, the critical buckling strain can be calculated. Mehar and Panda (2016a, b, 2018a) computed the vibration behavior, bending and dynamic response of FG reinforced CNT using shear deformation theory and finite element method. For the sake of generality, the mathematical model was presented with the mixture of Green Lagrange method. The convergence of these methodologies has been checked for the variety of results. The composite plates with different graded was investigated with isotropic and core phase. Avcar (2015) presented the separate and combined effects of rotary inertia, shear deformation and material non-homogeneity (MNH) on the values of natural frequencies of the simply supported beam. MNH is characterized considering the parabolic variations of Young's modulus and density along the thickness direction of the beam, while the value of

*Corresponding author, Ph.D., Research Scholar,
E-mail: muzamal45@gmail.com;
muzamalhussain@gcuf.edu.pk
[a] Professor

ISSN: 2287-237X (Print), 2287-2388 (Online)

Poisson's ratio is assumed to remain constant. The results are verified with the molecular dynamics (MD) simulation based on compass force field. This improved formula shows a significant error at the smaller diameters and higher aspect ratios. Mehar *et al*. (2017a, b, c, d) studied the frequency response of FG CNT and reinforced CNT using the simple deformation theory, finite element modeling, Mori-Tanaka scheme. They investigated a new frequency phenomenon with the combination of Lagrange strain, Green-Lagrange, for double curved and curved panel of FG and reinforced FG CNT. The charactrictics of sandwich and grades CNT was found with labeling the temperarure environ. The thermoelastic frequency of single shallow panel was determined using Mori-Tanake formulations. The research of these authors has opened a new frequency spectrum for other material researchers. Chavan and Lal (2017) presented the bending characteristic of single wall carbon nanotube reinforced functionally graded composite (SWCNTRC-FG) plates. The finite element implementation of bending analysis of laminated composite plate via well-established higher order shear deformation theory (HSDT). Selim (2010) performed vibrational behavior of SWCNT with compression stresses using multilayers. The motion equation was derived for the vibration analysis of SWCNTs using wave propagation. However, the outcomes of this research noted for various structures and the overall electronic and structural properties. Civalek *et al*. (2018) examined the present paper, rotary inertia and small size effects on the free vibration response of single-walled carbon nanotubes. The equations in motion and associated boundary conditions are obtained by using Hamilton's principle on the basis of modified couple stress and Rayleigh beam theories. Mehar and Panda (2018b) investigated the curved shell and CNT vibration with thermal environment using higher order deformation theory. This CNT was mixed with different configurations of the layers. The results have been verified with the earlier investigations. Ebrahimi and Habibi (2017) studied the nonlinear response of laminated functionally graded carbon nanotube reinforced composite (FG-CNTRC) plate under low-velocity impact based on the Eshelby-Mori-Tanaka approach in thermal conditions. The governing equations are derived based on higher-order shear deformation plate theory (HSDT) under von Kármán geometrical nonlinearity assumptions. Azrar *et al*. (2011) have explained the effect of vibration of these tubes on the length scale of many end conditions using TBM and nonlocal elasticity theory by solving the generalized nonlinear algebraic equations; higher and lower frequencies associated with eigen-modes are obtained. Emdadi *et al*. (2019) investigated the free vibration analysis of annular sandwich plates with various functionally graded (FG) porous cores and carbon nanotubes reinforced composite (CNTRC) facesheets based on modified couple stress theory (MCST) and first order shear deformation theories (FSDT). Mehar and Panda (2018c) investigated numerically the deflection behavior of carbon nanotubereinforced composite plate is using the finite element method and the result accuracy is established via threepoint experimental bending test data. Fazelzadeh and Ghavanloo (2012a, b) developed a nonlocal anisotropic elastic shell model to study the effect of small scale on shell-like vibration of single-walled carbon nanotubes (SWCNTs) with arbitrary chirality. Anisotropic elastic shell model is reformulated using the nonlocal differential constitutive relations of Eringen. Single-walled carbon nanotubes (SWCNTs) exhibit remarkable chirality-dependent mechanical phenomena. In present paper, an anisotropic elastic shell model is developed to study the vibration characteristics of chiral SWCNTs.

Rouhi *et al.* (2013) executed the axial buckling of double-walled CNT subject to various layer-wise conditions by using Rayleigh-Ritz based upon nonlocal Flügge shell theory. Their study showed that the number of different layer-wise boundary conditions dominates the choice of values for nonlocal parameter. Mehar and Panda (2018d) developed a general mathematical model for the evaluation of the theoretical flexural responses of the functionally graded carbon nanotube reinforced composite doubly curved shell panel using higher-order shear deformation theory with thermal load. Hussain and Naeem (2017) examined the frequencies of armchair tubes using Flügge's shell model. The effect of length and thickness-to-radius ratios against fundamental natural frequency with different indices of armchair tube was investigated. Mohammadimehr and Alimirzaei (2016) analyzed the nonlinear static and free vibration analysis of Euler-Bernoulli composite beam model reinforced by functionally graded single-walled carbon nanotubes (FG-SWCNTs) with initial geometrical imperfection under uniformly distributed load using finite element method (FEM) is investigated. The governing equations of equilibrium are derived. Rafiee and Moghadam (2012) employed a 3D-FEM with reinforced polymer CNT. The shear deformation of CNTs is implicated as using TBM and results are compared with earlier simulations. The behavior of reinforced polymer CNT is evaluated both in axial and transverse direction subject to high strain loading and impact of buckling are stimulated at micro-scale. Sofiyev and Avcar (2010) studied the stability of cylindrical shells that composed of ceramic, FGM, and metal layers subjected to axial load and resting on Winkler-Pasternak foundations. Hussain *et al*. (2017) demonstrated an overview of Donnell theory for the frequency characteristics of two types of SWCNTs. Fundamental frequencies with different parameters have been investigated with wave propagation approach. Mehar and Panda (2018e) reported the nonlinear finite solutions of the nonlinear flexural strength and stress behaviour of nano sandwich graded structural shell panel under the combined thermomechanical loading. Ansari and Rouhi (2013) summarized the effect of small scale, geometrical parameter and layer-wise end conditions of double-walled CNT by adopting Flügge shell model (FSM). They depicted that the continuum model considering the nonlocal effect compels the short double-walled CNT more flexible. Mehar *et al*. (2018a) evaluated the frequency behavior of nanolpate structure using FEM including the nonlocal theory of elasticity. Computer generated results are created by using the software first time robustly to check the vibration of nanoplate. The efficiency was checked by comparing the results of available data. Hussain and Naeem (2018a) used

Donnell's shell model to calculate the dimensionless frequencies for two types of single-walled carbon nanotubes. The frequency influence was observed with different parameters. Tohidi *et al*. (2018) considered an analysis into the nonlinear forced vibration of a micro cylindrical shell reinforced by carbon nanotubes (CNTs) with considering agglomeration effects. The structure is subjected to magnetic field and transverse harmonic mechanical load. In addition, Fereidoon *et al.* (2013) executed the 3D finite element method to find the modal analysis of reinforced polymer CNT with two type of edge condition. The frequencies obtained through finite element method showed a reasonable increment on comparing with neat polymer. Moghadam *et al.* (2014) scrutinized the frequencies of SWCNTs using molecular mechanics approach with various parameters. The frequency outcomes revealed the frequencies increases or decreases with the orientation of carbon-carbon bond.

Mehar *et al*. (2018b) studied the bending responses of nanotube-reinforced curved sandwich shell panel structure under the influence of the thermomechanical loading. Further, the temperature dependent material properties of the sandwich structure are assumed to evaluate the exact responses. Fatahi-Vajari *et al*. (2019) studied the vibration of single-walled carbon nanotubes based on Galerkin's and homotopy method.This work analyses the nonlinear coupled axial–torsional vibration of single-walled carbon nanotubes (SWCNTs) based on numerical methods. Two-second order partial differential equations that govern the nonlinear coupled axial–torsional vibration for such nanotube are derived. Madaini *et al.* (2016) studied the vibration of FG-CNT-reinforced piezoelectric cylindrical shells utilizing the method of differential quadrature. The mixture rule of four distribution types was used in the thickness direction. Asghar *et al*. (2019) conducted the vibration of nonlocal effect for double-walled carbon nanotubes using wave propagation approach. Many material parameters are varied for the exact frequencies of many indices of double-walled carbon nanotubes. Karami *et al.* (2017) conducted the analysis analysis of FG nanoplates, spherical nano particles and inisotropic nanoparticles using quasi-3D model, 3D elasticity and nonlocal theory. They investigated the dispersion analysis of FG nanoplates nonlocal strain gradient effect and triaxial magnetic effect. Avcar (2019) conducted the influence of various volume fraction laws using the classical theory for FG beam. By varying the volume fraction laws, the span-to-depth ratio versus frequencies was examined in detail. The frequencies for span to depth ratio with varying volume fraction index were examined in detail. Shahrma *et al*. (2019) studied the functionally graded material using sigmoid law distribution under hygrothermal effect. The Eigen frequencies are investigated in detail. Frequency spectra for aspect ratios have been depicted according to various edge conditions. Semmah *et al.* (2019) studied the buckling analysis of zigzag single walled boron nitride based on Winkler foundation. Effect of different nonlocal parameter was investigated with closed form solution. Recently Hussain and Naeem (2019a, b, c, d, 2020) and performed the vibration of SWCNTs based on wave propagation approach and Galerkin's method. They investigated many physical parameters for the rotating and non-rotating vibrations of armchair, zigzag and chiral indices. Moreover, the mass density effect of single-walled carbon nanotubes with in-plane rigidity have been calculated for zigzag and chiral indice.

The particular motivation of present work is to investigate the vibration characteristics of armchair, zigzag and chiral SWCNT by means of Kelvin's model based on wave propagation approach. The suggested method to investigate the solution of fundamental eigen relations is wave propagation approach (WPA), which is a well-known and efficient technique to develop the fundamental frequency equations. There is no evidence found in the literature regarding our work. The specific influence of four different end supports based on Kelvin's model such as clamped-clamped (C-C), and clamped-free supported (C-F) is examined in detail. Many material researchers calculated the frequency of CNTs using different techniques, for example, classical molecular dynamics (Han *et al.* 1997), Rayleigh-Ritz method (Swaddiwudhipong *et al.* 1995), continuum models (Duan *et al.* 2007), Galerkin's method (Elishakoff and Pentaras 2009), Raman spectroscopy (Jorio *et al.* 2001) deformation theory (Mehar *et al*. 2016), finite element method (Mehar *et al*. 2018c), Green–Lagrange strain field (Mehar *et al*. 2018c) and Multiscale modeling approach (Mehar and Panda 2019, Mehar *et al*. 2019). Also, the modified Kelvin's model based on the wave propagation approach for estimating orthotropic fundamental natural frequency has been developed to converge more quickly than other methods and models. A large use of tube structures in practical applications makes their theoretical analysis an important field of structural dynamics. Since a tube problem is a physical one, so their vibrational behaviors are distorted by variations of physical and material parameters. Effects of different parameters for in-plane rigidity (IPR) and mass density per unit lateral area (MDA) on the fundamental natural frequencies versus ratio of length-to-diameter have been investigated. In this paper, utilizing the Kelvin's model for the vibration of orthotropic carbon nanotubes provides a governing equation using wave propagation approach with C-C and C-F conditions. The effect of frequencies against length-to-diameter ratio/ aspect ratio by varying the in-plane rigidity mass per unit lateral area is studied. It has been shown that on enhancing bending rigidity for SWCNTs the frequency curves increase. It is observed that the outcomes of frequency response of armchair with prescribed boundary conditions are lower than that of zigzag frequency values and the outcomes of frequency response of chiral with prescribed boundary conditions are lower than that of zigzag frequency values. The presented orthotropic vibration modeling and analysis of carbon nanotubes may be helpful especially in applications such as oscillators and in non-destructive testing.

2. Materials and methods

When a graphene sheet is rolled with its hexagonal cells, the structure can be conceptualized as single-walled carbon

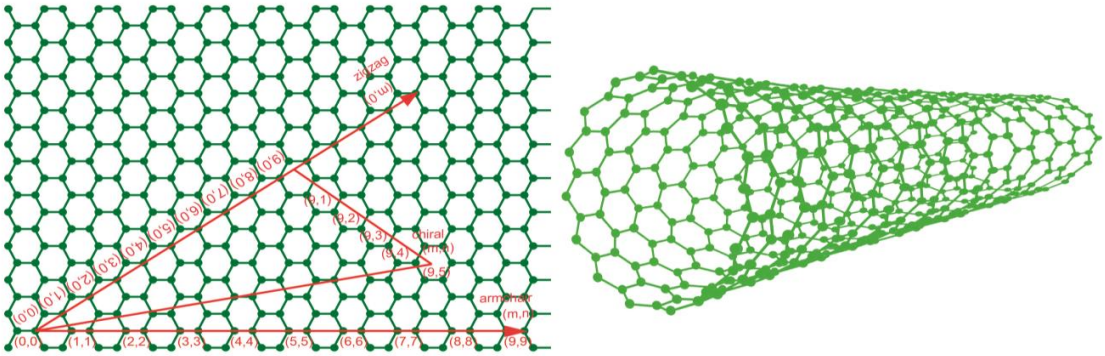

Fig. 1 Hexagonally description of armchair, zigzag and chiral SWCNTs on the graphene sheet

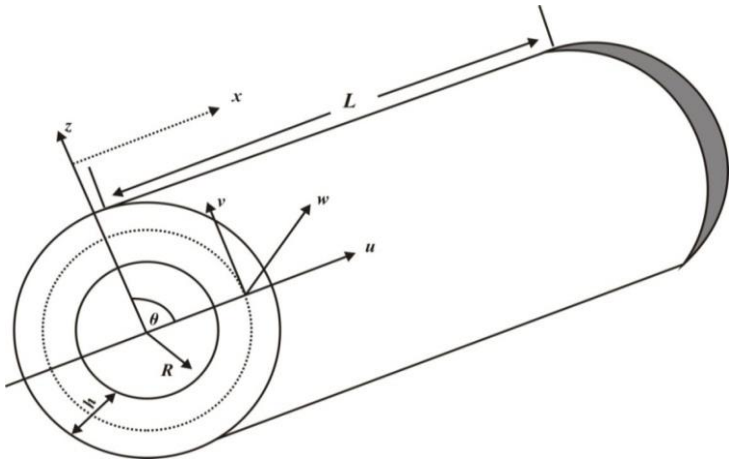

Fig. 2 Geometry of SWCNTs

nanotubes and its circumference and quantum properties depend upon the chirality and diameter described as a pair of (n, m). The indices pair occur during the rolling of tube Fig. 1 shows the schema of the pair indices as (m, n) which occurs on rolling of the tube and this pair of in indices formed as armchair, zigzag and chiral, if $m = n$, $n = 0$, if $m \neq n$, respectively. The geometry of SWCNTs is shown in Fig. 2.

2.1 Orthotropic Kelvin-like model

Over the past several years vibration of tube/shell and plate structures of various configurations and boundary conditions have been extensively studied (Hussain *et al.* 2018a, b, c, 2019a, b, 2020a, b, Hussain and Naeem 2018b, Asghar *et al.* 2020, Taj *et al.* 2020). The geometrical relations are given by Flugge's shell theory (Flugge 1973, Zou and Foster 1995, Paliwal *et al.* 1995). The coordinate system x, y and z are axial, circumferential and radial coordinates respectively whose dimensionless coordinates are $\alpha = x/R$, $\beta = y/R$ and $\gamma = z/R$ and ∇^2 is the Laplace operator.

Along α, β and γ directions, the displacement of middle surface is u, v and w, respectively

$$\varepsilon_\alpha = \frac{1}{R}\left(\frac{\partial u}{\partial \alpha} - \gamma\frac{\partial^2 w}{\partial \alpha^2}\right) \tag{1}$$

$$\varepsilon_\beta = \frac{1}{R}\left(\frac{\partial v}{\partial \beta} + w\right) - \frac{\gamma}{R(1+\gamma)}\left(\frac{\partial^2 w}{\partial \beta^2} + w\right) \tag{2}$$

$$\varepsilon_{\alpha\beta} = \frac{\gamma}{R(1+\gamma)}\left[\frac{\partial u}{\partial \beta} + \frac{\partial v}{\partial \alpha} + 2\gamma\left(\frac{\partial v}{\partial \alpha} - \frac{\partial^2 w}{\partial \alpha \partial \beta}\right) + \gamma^2\left(\frac{\partial v}{\partial \alpha} - \frac{\partial^2 w}{\partial \alpha \partial \beta}\right)\right] \tag{3}$$

The stress-strain relationships in dimensionless coordinates is as under (Gao and An 2010)

$$\sigma_\alpha - \nabla^2\sigma_\alpha = E_1(\varepsilon_\alpha + \mu_1\varepsilon_\beta)/(1 - \mu_1\mu_2) \tag{4}$$

$$\sigma_\beta - \nabla^2\sigma_\beta = E_2(\varepsilon_\beta + \mu_2\varepsilon_\alpha)/(1 - \mu_1\mu_2) \tag{5}$$

$$\tau_{\alpha\beta} - \nabla^2\tau_{\alpha\beta} = G\varepsilon_{\alpha\beta} \tag{6}$$

where σ_α, σ_β and $\tau_{\alpha\beta}$ are normal and shear stresses, and ε_α, ε_β and $\varepsilon_{\alpha\beta}$ are respective strains; E_1 and E_2 are moduli of elasticity; Poisson's ratios in the directions of α and β are μ_2 and μ_1 respectively. G is modulus of rigidity or shear modulus. Also, we have $E_1\mu_1 = E_2\mu_2$ and $\nabla^2 = (\partial^2/\partial\alpha^2 + \partial^2/\partial\beta^2)/R^2$ which is the Laplace operator in dimensionless coordinates. The element of tube in our coordinates is shown in Fig. 3, where (N, S, Q) are

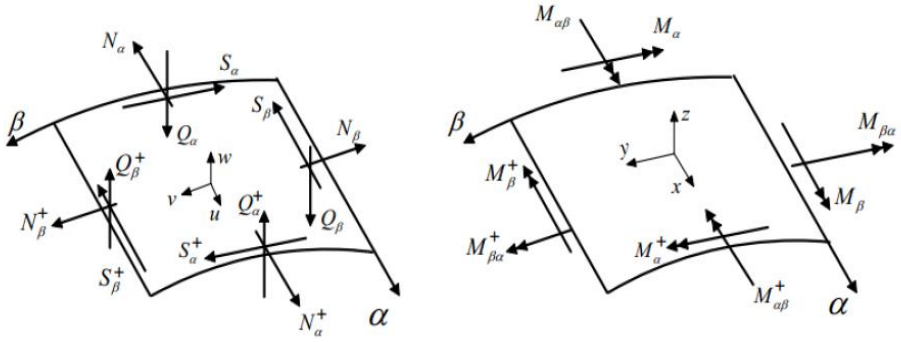

Fig. 3 Resolution of components of stress and moments of the middle surface of CNTs

the stress resultants and (M) is the moment. The thermal expansion causes pre-stress, which is neglected due to the reference temperature. We arrive at the dynamic equilibrium equations

$$\begin{cases} \dfrac{\partial N_\alpha}{\partial \alpha}+\dfrac{\partial S_\beta}{\partial \beta}+\kappa=\rho hR\dfrac{\partial^2 u}{\partial t^2} \\ \dfrac{\partial N_\beta}{\partial \beta}+\dfrac{\partial S_\alpha}{\partial \alpha}+Q_\beta=\rho hR\dfrac{\partial^2 v}{\partial t^2} \\ \dfrac{\partial Q_\alpha}{\partial \alpha}+\dfrac{\partial Q_\beta}{\partial \beta}+N_\beta=\rho hR\dfrac{\partial^2 w}{\partial t^2} \end{cases} \tag{7}$$

$$\begin{cases} \dfrac{\partial M_{\alpha\beta}}{\partial \alpha}+\dfrac{\partial M_\beta}{\partial \beta}-RQ_\beta=0 \\ \dfrac{\partial M_{\beta\alpha}}{\partial \beta}+\dfrac{\partial M_\alpha}{\partial \alpha}-RQ_\alpha=0 \end{cases} \tag{8}$$

where ρ is the mass density.

The resultants (N,S,Q) are derived from above set of integral equations using the stress components.

$$(1-\nabla^2)\begin{bmatrix} N_\alpha, S_\alpha, \\ M_\alpha, M_{\alpha\beta} \end{bmatrix}=\int_{-\frac{h}{2}}^{\frac{h}{2}}\begin{bmatrix} \sigma_\alpha, \tau_{\alpha\beta}, \\ z\,\sigma_\alpha, z\,\tau_{\alpha\beta} \end{bmatrix}\left(1+\frac{z}{R}\right)dz \tag{9}$$

$$(1-\nabla^2)\begin{bmatrix} N_\beta, S_\beta, \\ M_\beta, M_{\beta\alpha} \end{bmatrix}=\int_{-\frac{h}{2}}^{\frac{h}{2}}\begin{bmatrix} \sigma_\beta, \tau_{\beta\alpha}, \\ z\,\sigma_\beta, z\,\tau_{\beta\alpha} \end{bmatrix}dz \tag{10}$$

$$(1-\nabla^2)\left(Q_\alpha, Q_\beta\right)=\int_{-\frac{h}{2}}^{\frac{h}{2}}\left[\tau_{\alpha z}, \tau_{\beta z}\right]dz \tag{11}$$

where h is thickness of the shell. Above equations result in

$$N_\alpha-\nabla^2 N_\alpha=\frac{K}{R}\left[\frac{\partial u}{\partial \alpha}+\mu_1\left(\frac{\partial v}{\partial \beta}+w\right)-c^2\frac{\partial^2 w}{\partial \alpha^2}\right] \tag{12}$$

$$N_\beta-\nabla^2 N_\beta=\frac{Kk_1}{R}\left[\frac{\partial v}{\partial \beta}+\mu_2\frac{\partial u}{\partial \alpha}+w+c^2\left(\frac{\partial^2 w}{\partial \beta^2}+w\right)\right] \tag{13}$$

$$S_\alpha-\nabla^2 S_\alpha=\frac{Kk_2}{R}\left[\frac{\partial u}{\partial \beta}+\frac{\partial v}{\partial \alpha}-c^2\left(\frac{\partial^2 w}{\partial \alpha\partial \beta}-\frac{\partial v}{\partial \alpha}\right)\right] \tag{14}$$

$$S_\beta-\nabla^2 S_\beta=\frac{Kk_2}{R}\left[\frac{\partial u}{\partial \beta}+\frac{\partial v}{\partial \alpha}+c^2\left(\frac{\partial^2 w}{\partial \alpha\partial \beta}+\frac{\partial v}{\partial \alpha}\right)\right] \tag{15}$$

$$M_\alpha-\nabla^2 M_\alpha=-Kc^2\left[\frac{\partial u}{\partial \alpha}+\mu_1\frac{\partial v}{\partial \beta}-\left(\frac{\partial^2 w}{\partial \alpha^2}+\mu_1\frac{\partial^2 w}{\partial \beta^2}\right)\right] \tag{16}$$

$$M_\beta-\nabla^2 M_\beta=Kk_1c^2\left(\frac{\partial^2 w}{\partial \beta^2}+w+\mu_2\frac{\partial^2 w}{\partial \alpha^2}\right) \tag{17}$$

$$M_{\alpha\beta}-\nabla^2 M_{\alpha\beta}=2Kk_2c^2\left(\frac{\partial v}{\partial \alpha}-\frac{\partial^2 w}{\partial \alpha\partial \beta}\right) \tag{18}$$

$$M_{\beta\alpha}-\nabla^2 M_{\beta\alpha}=Kk_2c^2\left(\frac{\partial u}{\partial \beta}-\frac{\partial v}{\partial \alpha}+2\frac{\partial^2 w}{\partial \alpha\partial \beta}\right) \tag{19}$$

$$Q_\alpha-\nabla^2 Q_\alpha=\frac{Kc^2}{R}\begin{bmatrix} \dfrac{\partial^2 u}{\partial \alpha^2}-k_2\dfrac{\partial^2 u}{\partial \beta^2}+(k_2+\mu_1)\dfrac{\partial^2 v}{\partial \alpha\partial \beta}- \\ \dfrac{\partial^3 w}{\partial \alpha^3}-(2k_2+\mu_1)\dfrac{\partial^3 w}{\partial \alpha\partial \beta^2} \end{bmatrix} \tag{20}$$

$$Q_\beta-\nabla^2 Q_\beta=\frac{Kk_1c^2}{R}\begin{bmatrix} 2\dfrac{k_2}{k_1}\dfrac{\partial^2 v}{\partial \alpha^2}-\dfrac{\partial^3 w}{\partial \beta^3}- \\ \dfrac{\partial w}{\partial \beta}-\left(2\dfrac{k_2}{k_1}+\mu_2\right)\dfrac{\partial^3 w}{\partial \alpha^2\partial \beta} \end{bmatrix} \tag{21}$$

where $K=E_1h/(1-\mu_1\mu_2)$, $k_1=E_2/E_1$, $k_2=G(1-\mu_1\mu_2)/E_1$, $c^2=h_o^3/(12R^2h)$.

Using Eqs. (7) and (8), we get Kelvin-like orthotropic elastic shell model.

The obtained model is as follows

$$\begin{aligned} &\left[\frac{\partial^2}{\partial \alpha^2}+k_2(1+c^2)\frac{\partial^2}{\partial \beta^2}\right]u+\left[(\mu_1+k_2)\frac{\partial^2}{\partial \alpha\partial \beta}\right]v \\ &+\left[6+\frac{\partial}{\partial \alpha}+c^2\left(k_2\frac{\partial^3}{\partial \alpha\partial \beta^2}-\frac{\partial^3}{\partial \alpha^3}\right)\right]w \\ &=\frac{\rho hR^2[1-\nabla^2]}{K}\frac{\partial^2 u}{\partial t^2} \end{aligned} \tag{22}$$

$$\begin{aligned} &\left[(\mu_1+k_{\,2})\frac{\partial^2}{\partial \alpha\partial \beta}\right]u+\left[k_2(1+3c^2)\frac{\partial^2}{\partial \alpha^2}+k_1\frac{\partial^2}{\partial \beta^2}\right]v \\ &+\left[k_1\frac{\partial}{\partial \beta}-c^2(\mu_1+3k_2)\frac{\partial^3}{\partial \alpha^2\partial \beta}\right]w \\ &=\frac{\rho hR^2[1-\nabla^2]}{K}\frac{\partial^2 v}{\partial t^2} \end{aligned} \tag{23}$$

$$\left[\mu_1\frac{\partial}{\partial\alpha}-c^2\left(\frac{\partial^3}{\partial\alpha^3}-k_2\frac{\partial^3}{\partial\alpha\partial\beta^2}\right)\right]u$$
$$+\left[k_1\frac{\partial}{\partial\beta}-c^2(\mu_1+3k_2)\frac{\partial^3}{\partial\alpha^2\partial\beta}\right]v$$
$$+\left[\left(1+\frac{1}{c^2}\right)k_1+\frac{\partial^4}{\partial\alpha^4}+k_1\frac{\partial^4}{\partial\beta^4}+2k_1\frac{\partial^2}{\partial\beta^2}\right.$$
$$\left.+(2\mu_1+4k_2)\frac{\partial^4}{\partial\alpha^2\partial\beta^2}\right]c^2w+\frac{R^2}{K}(1-\nabla^2)\left[Ew+\eta\frac{\partial w}{\partial t}\right]$$
$$=-\frac{\rho hR^2[1-\nabla^2]}{K}\frac{\partial^2 w}{\partial t^2} \quad (24)$$

where $K=\frac{\mathrm{E_1h}}{1-\mu_1\mu_2}$, medium has stiffness E, and the viscosity of the medium is η. Two kinds of boundary conditions may be assumed while solving such problems. These three conditions are:

Clamped-clamped

$$\alpha=\beta=\gamma=\frac{\partial\gamma}{\partial\alpha}=0, \quad \text{at} \quad \alpha=0,\alpha=L/R \quad (25)$$

Clamped-free

$$\begin{cases}\alpha=\beta=\gamma=\dfrac{\partial\gamma}{\partial\alpha}=0 & \text{at} \quad \alpha=0\\ N_{\alpha\alpha}=M_{\alpha\alpha}=N_{\alpha\beta}=M_{\alpha\beta=}0 & \text{at} \quad \alpha=L/R\end{cases} \quad (26)$$

where L is the length of CNTs.

Using any combination of above three conditions we come close to nonlocal Flugge's shell model. Above system of equations is the nonlocal orthotropic Kelvin-like shell model for CNTs. To understand the waves propagating in CNTs, we need to derive the dispersion relations.

2.2 Application of wave propagation approach

The solutions of wave system of Eqs. (22)-(24) for axisymmetric waves is given by (Wang and Gao 2016).

$$\begin{cases}u(\alpha,t)=U\mathrm{e}^{ik\left(\alpha-\frac{\nu t}{R}\right)}\\ v(\alpha,t)=V\mathrm{e}^{ik\left(\alpha-\frac{\nu t}{R}\right)}\\ w(\alpha,t)=W\mathrm{e}^{ik\left(\alpha-\frac{\nu t}{R}\right)}\end{cases} \quad (27)$$

where U, V and W are the amplitudes of waves along the direction of x, y and z respectively, the dimensionless wave vector in the longitudinal direction is $k=\frac{\pi\mathrm{mR}}{\mathrm{L}}$, in longitudinal direction m,ν is the half axial wave number and wave phase velocity.

Substituting Eq. (27) in system of Eqs. (22)-(24) and simplifying, in matrix form, we get the following system

$$[M^{(1)}(k,\nu)]_{3\times3}\begin{bmatrix}U\\V\\W\end{bmatrix}=[0\quad 0\quad 0]^T \quad (28)$$

For the nontrivial solution of above equation, we have

$$Det\left[M^{(1)}(k,\nu)\right]=0 \quad (29)$$

Table 1 Convergence of present Kelvin's model frequencies of SWCNTs with Ref. (Heydarpour *et al.* 2014)

m	ν	Kelvin's theory	Heydarpour *et al.* (2014)	Present
0	0.12	7	0.6240	0.6228
		9	0.6240	0.6234
		11	0.6240	0.6239
	0.17	7	0.8157	0.8143
		9	0.8157	0.8152
		11	0.8157	0.8155
	0.28	7	0.8553	0.8541
		9	0.8553	0.8547
		11	0.8553	0.8550

Table 2 Convergence of present Kelvin's model frequencies SWCNTs frequencies for parameters $\Delta=\omega R\sqrt{(1-\nu^2)\rho/E}$ with Swaddiwudhipong *et al.* (1995)

L/R	m	Method	⇂			
			1	2	3	4
20	1	Swaddiwudhipong *et al.* (1995)	0.016101	0.00545	0.00504	0.008534
		Present	0.016103	0.00545	0.00505	0.008536
0.25	1	Swaddiwudhipong *et al.* (1995)	0.95193	0.93446	0.90673	0.87076
		Present	0.95194	0.93446	0.90674	0.87078

3. Results and discussion

A methodology for constructing the modified Kelvin's theory based on wave propagation approach of single-walled CNTs for vibration analysis has been presented with the prescribed boundary conditions as: C-C and C-F. For the accuracy of present model, the frequencies of SWCNTs are well matched with the earlier published results. Since the percentage of error is negligible, the model is concluded as valid. The following material parameters are as, the ratio of Young's modulus and mass density, the in-plane stiffness or rigidity, Poisson's ratio E/ρ = 3.6481 × 10^8 m^2/s^2, Eh = 278.25 GPa·nm, ν = 0.2, respectively (Zhang *et al.* 2009). The presented results are compared with Heydarpour *et al.* (2014) and Swaddiwudhipong *et al.* (1995) in Tables 1, 2 and for the validation with the experimental results (Jorio *et al.* 2001) as shown in Table 3. The percentage error of present results is in the acceptable range with ±5%. We can observe the present results of Kelvin's model having good coherence with Heydarpour *et al.* (2014), Swaddiwudhipong *et al.* (1995) and Jorio *et al.* (2001).

Now the results for armchair, zigzag and chiral are discussed in detail with the present Kelvins model. For armchair frequencies computations of C-C and C-F BCs is obtained with varying index 10~20 and L/d = 4.86~35.53. The fundamental natural frequencies (THz) of presented BCs are noted as 0.97293 to 0.011812 and 0.76587 to 0.01640, respectively, as shown in Figs. 4-6. Now the study

Table 3 Convergence of present Kelvin's model with experimental model of Jorio *et al*. (2001)

	f (THz)							
(*m*, *n*)	(8, 7)	(10, 5)	(11, 4)	(14, 1)	(18, 0)	(17, 2)	(11,11)	(12, 12)
Jorio *et al*. (2001)	7.165	7.105	6.865	6.295	5.276	5.216	4.917	4.527
Present	7.018	7.093	5.781	6.103	5.161	5.142	4.805	4.465
Difference %	1.42	1.49	3.85	1.92	1.76	1.83	1.87	1.71

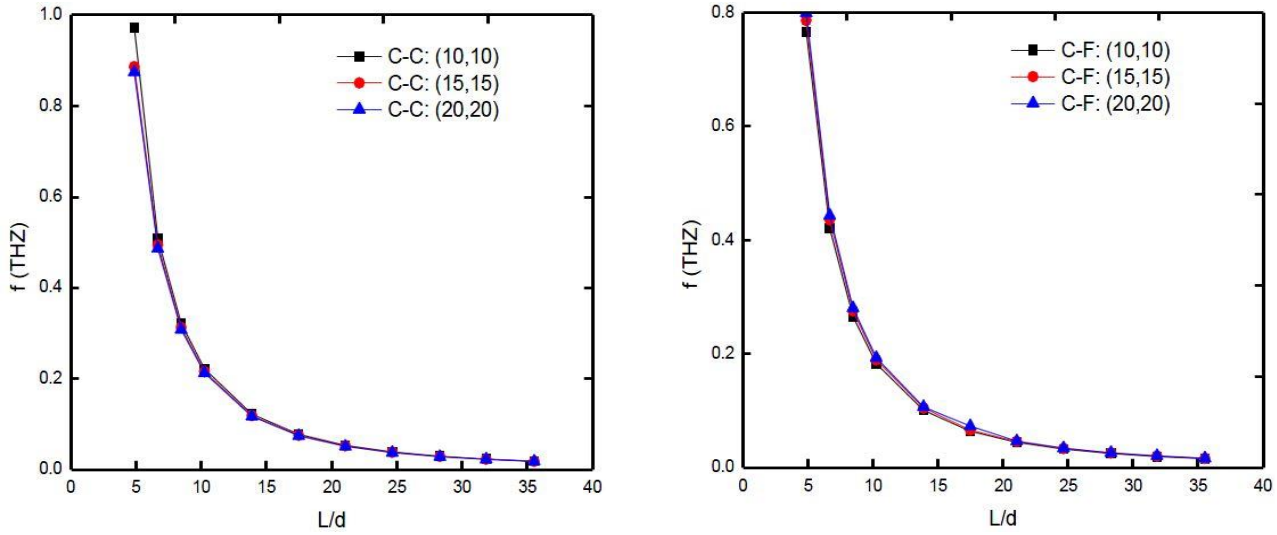

Fig. 4 Frequencies of armchair (10, 10), (15, 15), (20, 20) SWCNTs versus *L/d*

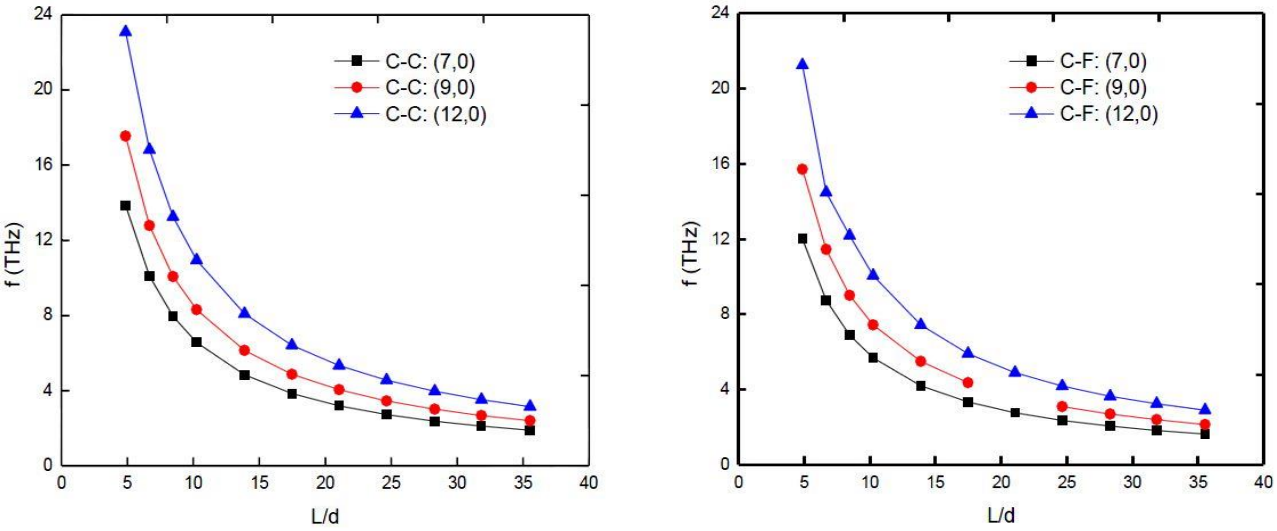

Fig. 5 Frequencies of zigzag (7, 0), (9, 0), (12, 0), SWCNTs versus *L/d*

is shifted to six zigzag tube measurement based on wave propagation approach by changing index 7~12, keeping ratios L/d fixed with BCs. The data set points of C-C (C-F) are obtained from 13.855~3.1585 THz (2.007~2.9058 THz) using present approach as shown in the Fig. 5. In all of these modes, (7, 0), the cross sections do not deform significantly from the nearly circular perimeter. So, for the other zigzag case (9, 0) and (12, 0), the natural frequencies increase, the axial and circumferential directions develop and become more visible. For chiral SWCNTs, with same length-to-diameter ratio, varying the chiral index as (6, 4), (9, 3), and (16, 4), it is observed that the frequency curve for chiral index (16, 7) is composed between (6, 4) and (9, 3). The computations for index (6, 4), are found to be 1.853 to 0.044 0.97293 to 0.011812 THz (1.413 to 0.032 THz), for index (9, 3) as 4.369 to 0.161 THz (3.875 to 0.130THz) and for index (16, 7) as 3.222 to 0.094 THz (2.970 to 0.083 THz), respectively, as shown in Fig. 6. Figs. 7-8 contain the frequencies in THz for in-plane rigidity of SWCNTs against the ratio of length-diameter *L/d*. These figures exhibit that

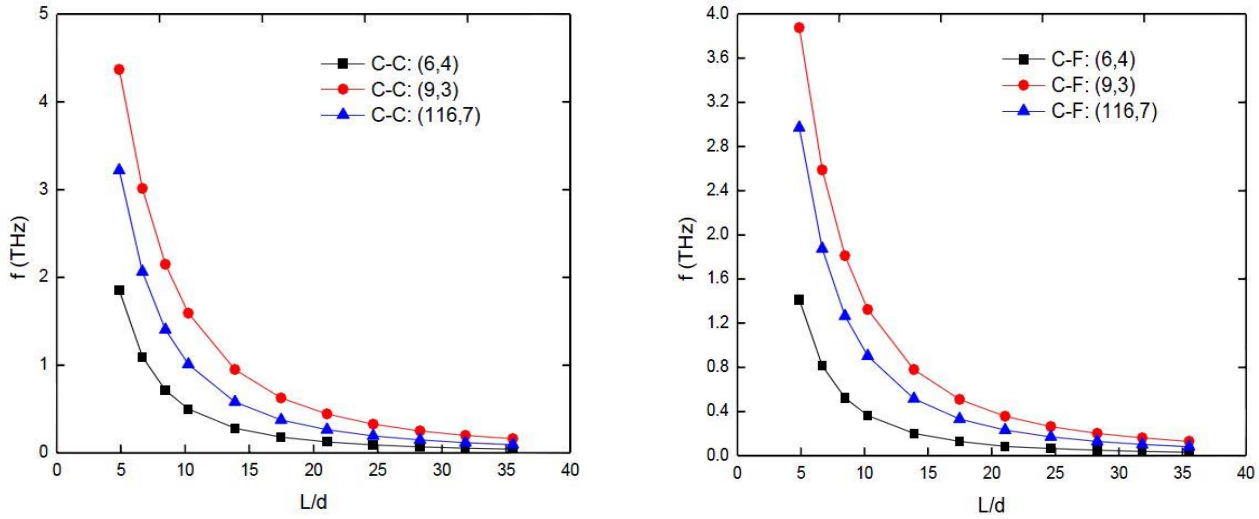

Fig. 6 Frequencies of chiral (6, 4), (9, 3), (16, 7), SWCNTs versus *L/d*

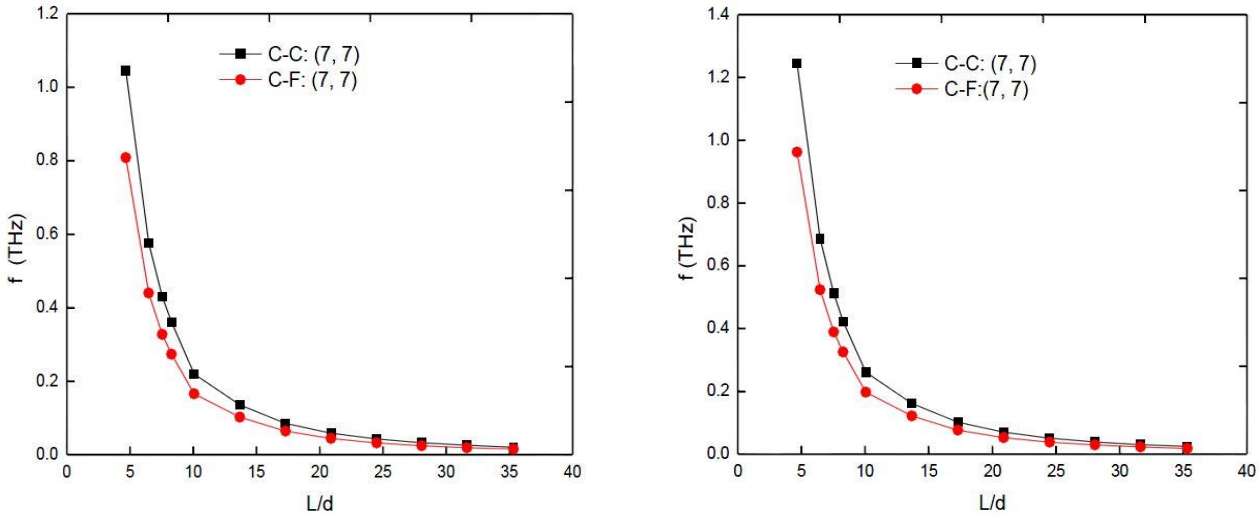

(a) (b)

Fig. 7 Frequencies of armchair (7, 7) SWCNTs versus *L/d* with *Eh* (a) 300 GPa.nm; (b) 425 GPa.nm

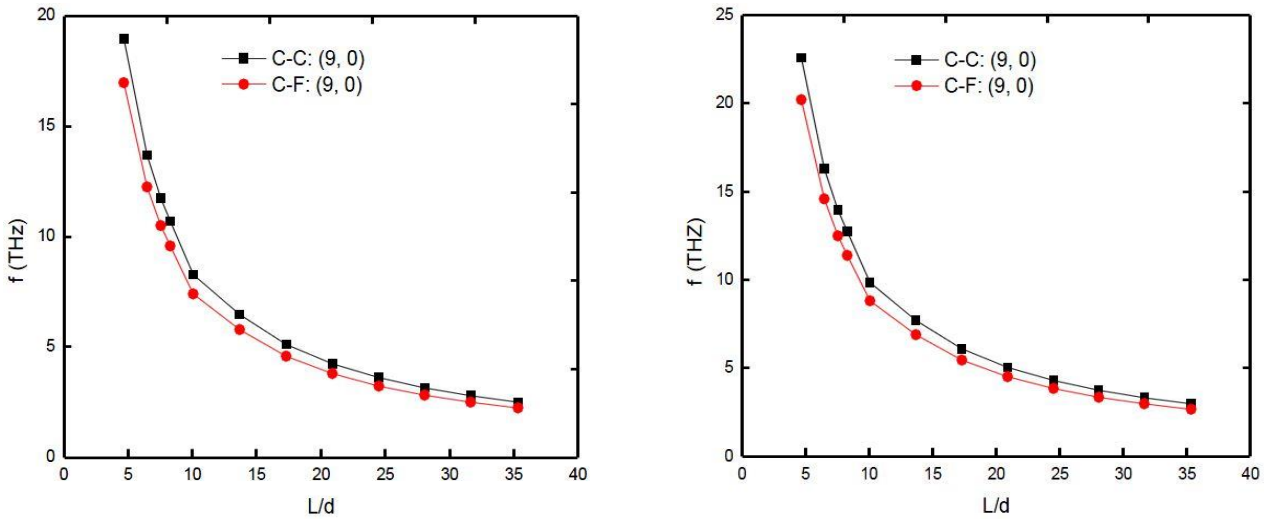

(a) (b)

Fig. 8 Frequencies of zigzag (9, 0) SWCNTs versus *L/d* with *Eh* (a) 300 GPa.nm; (b) 425 GPa.nm

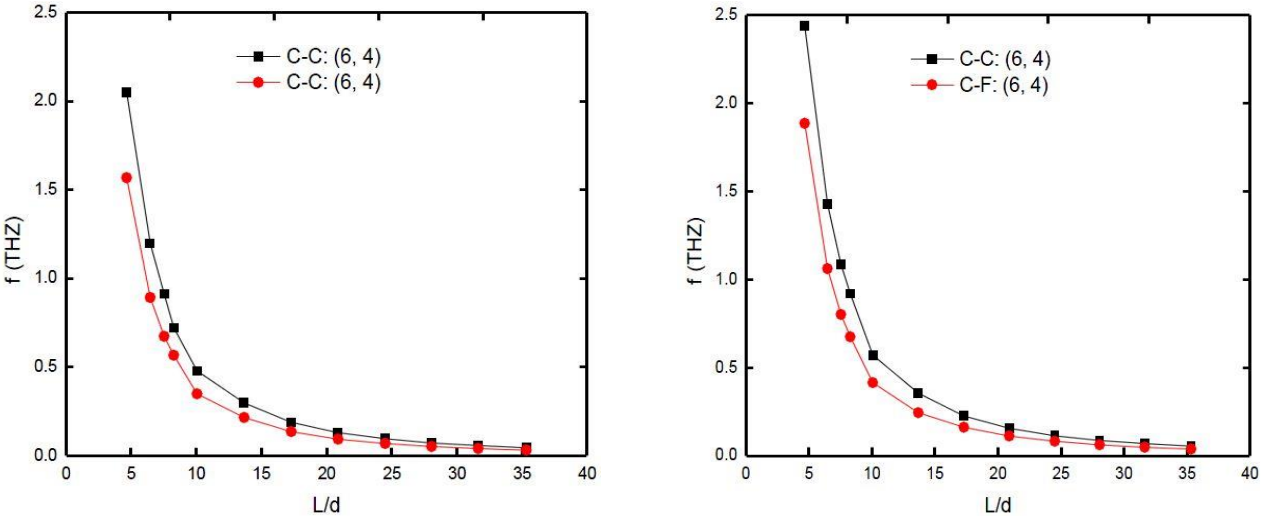

(a) (b)

Fig. 9 Frequencies of chiral (6, 4) SWCNTs versus *L/d* with *Eh* (a) 300 GPa.nm; (b) 425 GPa.nm

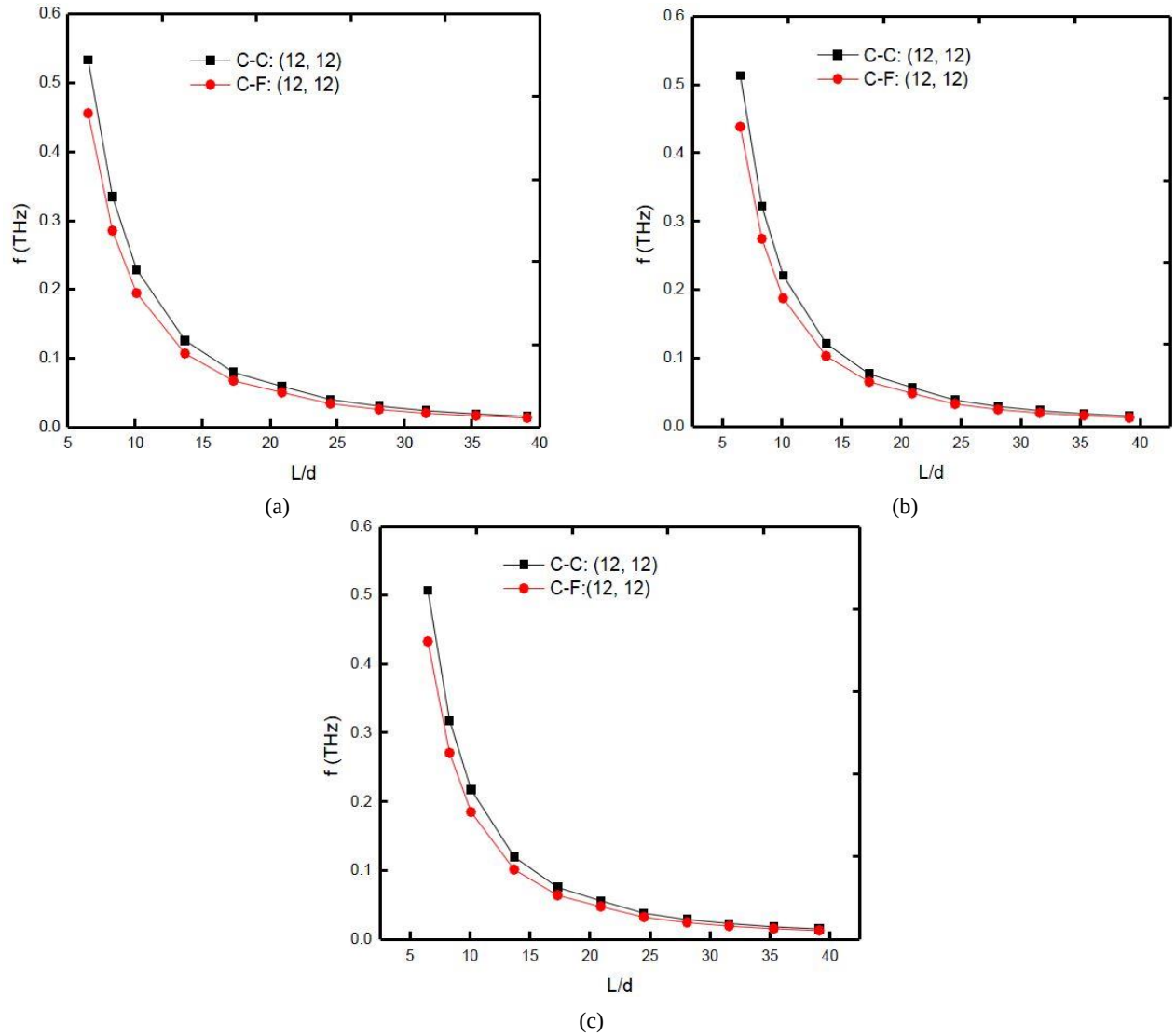

(a) (b)

(c)

Fig. 10 Frequencies of zigzag (12, 12) SWCNTs versus *L/d* with *ρh* (a) 740.52 nm; (b) 800.64 nm; (c) 820.80 nm

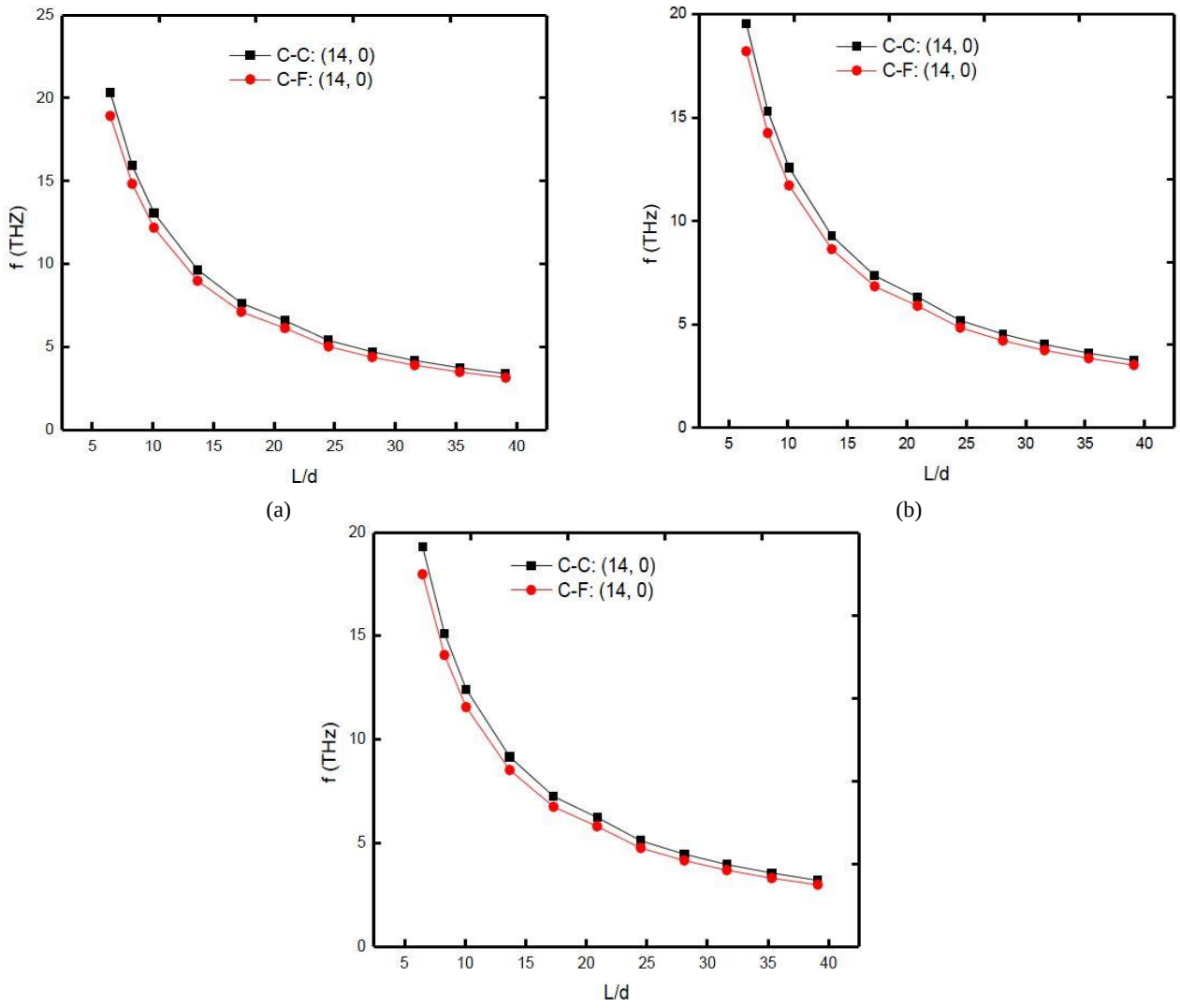

Fig. 11 Frequencies of zigzag (14, 0) SWCNTs versus *L/d* with (a) 740.52 nm; (b) 800.64 nm; (c) 820.80 nm

in-plan rigidity *Eh* varying from 300 GPa·nm ~425. Natural frequencies of SWCNTs for the category armchair (7, 7) and zigzag (9, 0) with specified boundary conditions using WPA are plotted against the length-diameter ratio, respectively. An interesting phenomenon can be seen from Figs. 6-7, that the fundamental natural frequency of zigzag (9, 0) SWCNTs are substantially larger than that of armchair (7, 7) SWCNTs. It is mentioned that the frequencies with boundary condition increase with an increase in IPR (*Eh)* and fundamental frequency decrease as *L*/*d* increase. The main result of the fundamental natural frequency (THz) at *Eh* = 300 GPa.nm for armchair (7, 7) as C-C (C-F) = 1.04524 (0.80828) increases to C-C (C-F) = 1.24408 (0.9620) at *Eh* = 425 GPa.nm, *L/d* = 4.67 as shown in Fig. 7 and at *Eh* = 425 GPa.nm for zigzag (9, 0) as C-C (C-F) = 18.963 (16.967) increases to C-C (C-F) = 22.570 (20.185) at *Eh* = 425 GPa.nm keeping *L/d* fixed as shown in Fig. 7.

Furthermore, the main result of the frequency (THz) at *Eh* = 300 GPa.nm for armchair (7, 7) as C-C (C-F) = 0.020594 (0.01547) slightly changes to 0.02451 (0.01842) at *Eh* = 425 GPa.nm and *L/d* = 4.67 as shown in Fig. 7 and at *Eh* = 425 GPa.nm for zigzag (9, 0) as C-C (C-F) = 2.5059 (2.2421) increases to C-C (C-F) = 2.9826 (2.6686) at *Eh* = 425 GPa.nm keeping *L/d* fixed as shown in Fig. 8. It is observed that with the slight increase in *L/d*, the frequencies for both armchair and zigzag decreases constantly instead for higher values of *Eh*. Fig. 9 shows the variation of frequencies with the effect of in-plane rigidity of chiral SWCNTs versus *L/d*. Also, in these figures as above discussed in the case of zigzag and chiral, in-plane rigidity *Eh* varying from 300 GPa·nm ~425 GPa·nm. The computed frequencies C-C and C-F BCs are presented with proposed model based on FSM. It can be seen that for smaller ratio, the frequencies are more significant and prominent. For example, with the end condition, as C-C (C-F) = (6, 4) *f*~2.048 (1.568) at *Eh* = 300 GPa.nm increases to C-C (C-F) = (6, 4) *f*~2.438 (1.866) at *Eh* = 425 GPa.nm for chiral SWCNTs as shown in Fig. 9. It is important to note that the fundamental natural frequencies of clamped-clamped for all indices are normally over-predicting than clamped-free. These figures show the aspect ratios with frequencies for in-

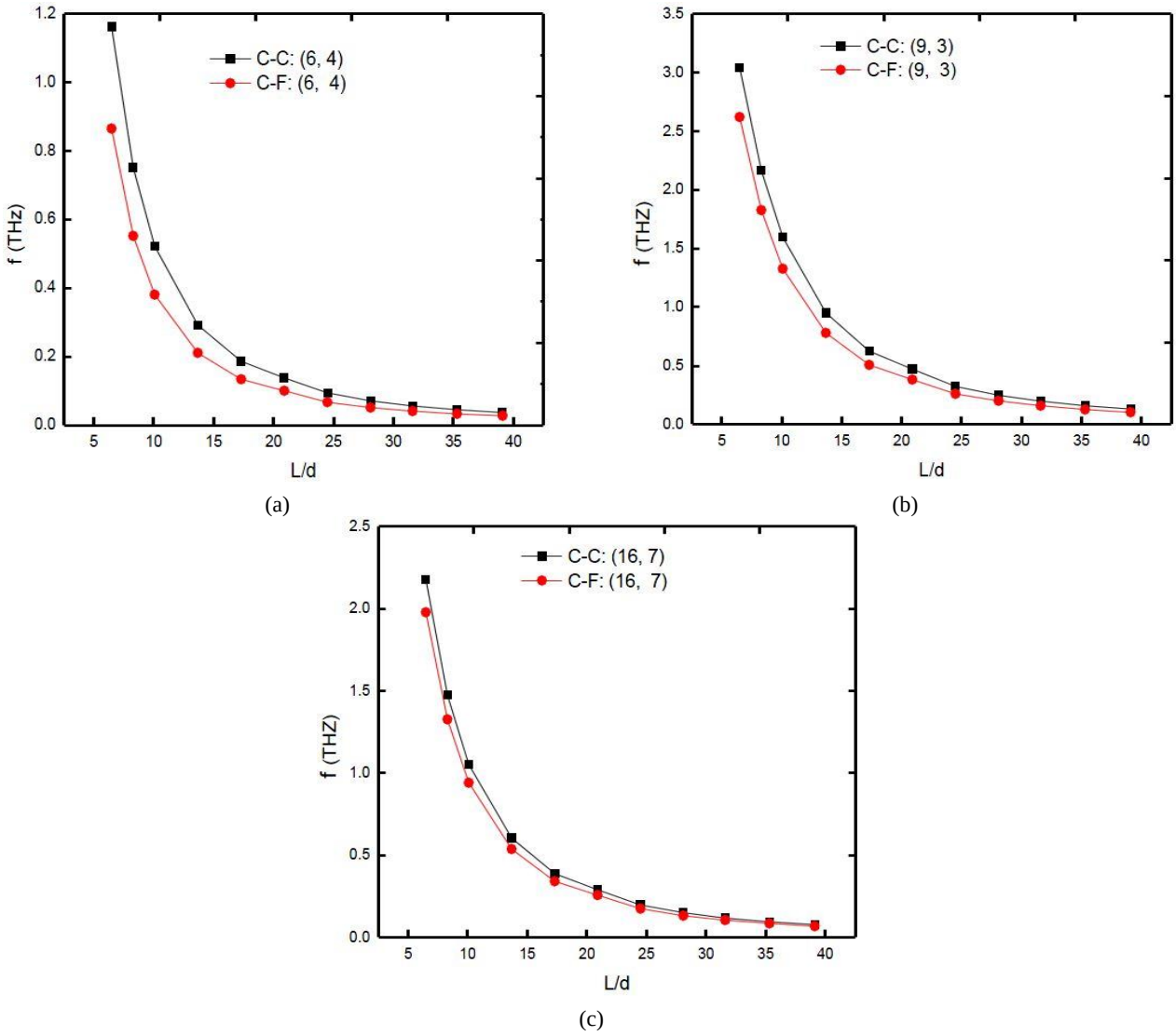

Fig. 12 Frequencies of chiral (6, 4), (9, 3), (16, 7) SWCNTs versus *L/d* with ρh = 740.52 nm

plane rigidity *Eh* = 300~425 GPa.nm. A trend of increasing frequencies of indices is as (9, 3) > (16, 7) > (6, 4). The chiral frequency decreases constantly instead for higher values of *Eh* with the slight increase in *L/d*, the frequencies for Figs. 10-11 exhibit the variation of C-C and C-F frequency for the case of the MDA (ρh). Results show that due to variation of MDA on frequency decreases considerably where the phenomena remain same for the in-plane rigidity case with same end conditions. In these figures, variation of armchair (12, 12) and zigzag (14, 0) is plotted for different values of ρh = 740.52 nm, 800.64 nm and 820.80 nm under prescribed boundary conditions. The fundamental natural frequencies for armchair tubes at ρh = 740.52 nm, C-C (C-F) = (12, 12) *f*~0.53352 (0.45575) decreases to C-C (C-F) = (12, 12) *f*~0.50676 (0.43289) at ρh = 820.80 nm and also at ρh = 820.64 nm decreases to C-C (C-F) = (12, 12) *f*~0.50676 (0.43289) for *L/d* = 6.5, as shown in Fig. 9 and for zigzag SWCNTs at ρh = 740.52 nm C-C (C-F) = (14, 0) *f* (THz) ~ 20.325 (18.923) decreases at ρh = 820.80 nm C-C (C-F) = (14, 0) *f*~19.3057 (17.974) and at ρh = 820.64 nm, C-C (C-F) = (14, 0) *f*~19.3057 (17.974) and *L/d* = 6.5 as shown in Fig. 10. It is observed that for all the cases, with increasing in ρh the resulting fundamental natural frequencies decrease.

Figs. 12-14 show the length-to-diameter ratios with frequencies for different values of ρh = 740.52 nm, 800.64 nm and 820.80 nm. It is noted that, with the increasing of ratio of length/diameter and ρh, the frequencies decreases of the CNTs as C-C (C-F) = (6, 4) *f*~1.162 (0.865) , C-C (C-F) = (9, 3) *f*~3.162 (2.723), C-C = (16, 7) *f*~2.178 (1.979) at ρh = 740.52 nm decreases to C-C (C-F) = (6, 4) *f*~1.118 (0.832), C-C (C-F) = (9, 3) *f*~1.103 (0.821), C-C (C-F) = (16, 7) *f*~3.003 (2.586) at ρh = 800.64 nm for decreases to C-C (C-F) = (6, 4) *f*~3.043 (2.621), C-C (C-F) = (9, 3) *f*~2.096 (1.9048), C-C (C-F) = (16, 7) *f*~2.068 (1.879) at ρh = 820.80 nm for chiral SWCNTs and *L/d* = 6.5 as shown in Figs. 10-12. In these figures, a reasonable decline in curve suggests that frequencies decrease with increase in MDA ρh = 740.52 nm to 820.80 nm. From our results, one can easy conclude that the declined in frequencies for MDA curves (6, 4), (9, 3) & (16, 7) is as follows (6, 4) < (16, 7) < (9, 3). Interestingly, in all cases C-F frequency curves are

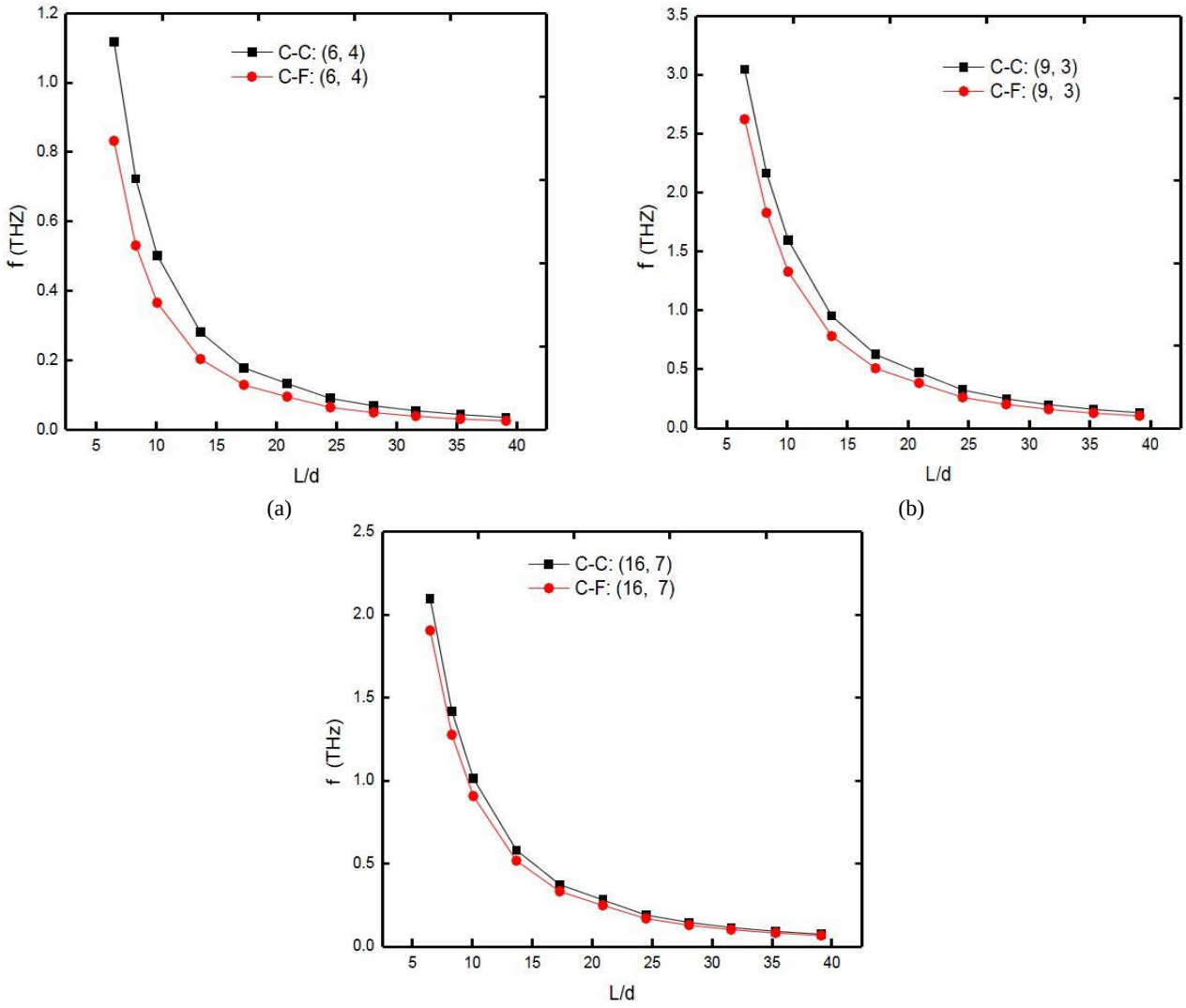

Fig. 13 Frequencies of chiral (6, 4), (9, 3), (16, 7) SWCNTs versus L/d with ρh = 800.64 nm

lower than C-C, but follow the same pattern as discussed earlier. Also, the frequency for shorter tube ratio is more significant.

4. Conclusions

In this paper attempts have been made to find the vibrational behavior of SWCNTs based on Kelvin's model by using wave propagation approach under C-C and C-F boundary conditions. It is concluded that from this type of analysis that CNTs behave like shell structure. The fundamental natural frequency of SWCNTs versus ratio of length-to-diameter for a wide range has been reported and investigated through the study with specified boundary conditions. Armchair, zigzag and chiral structures are considered for the vibrational analysis to investigate the effect of different mode and in-plane rigidity with end conditions. Moreover, the influence of MDA on the same structure is also developed. It is also concluded that the fundamental frequencies of zigzag and chiral tubes are greater than that of armchair tubes frequencies. In addition, by increasing three different value of IPR resulting frequencies also increase and frequencies decrease on increasing mass density per unit lateral area. Though the trends of frequency values of both MDA and IPR are converse to each other. By considering present model based on the Winkler and Pasternak foundations, the vibration characteristics of SWCNTs can be studied.

Declaration of Conflicting Interests

The author(s) declared no potential conflicts of interest with respect to the research, authorship, and/or publication of this article.

Funding

The author(s) received no financial support for the research, authorship, and/or publication of this article.

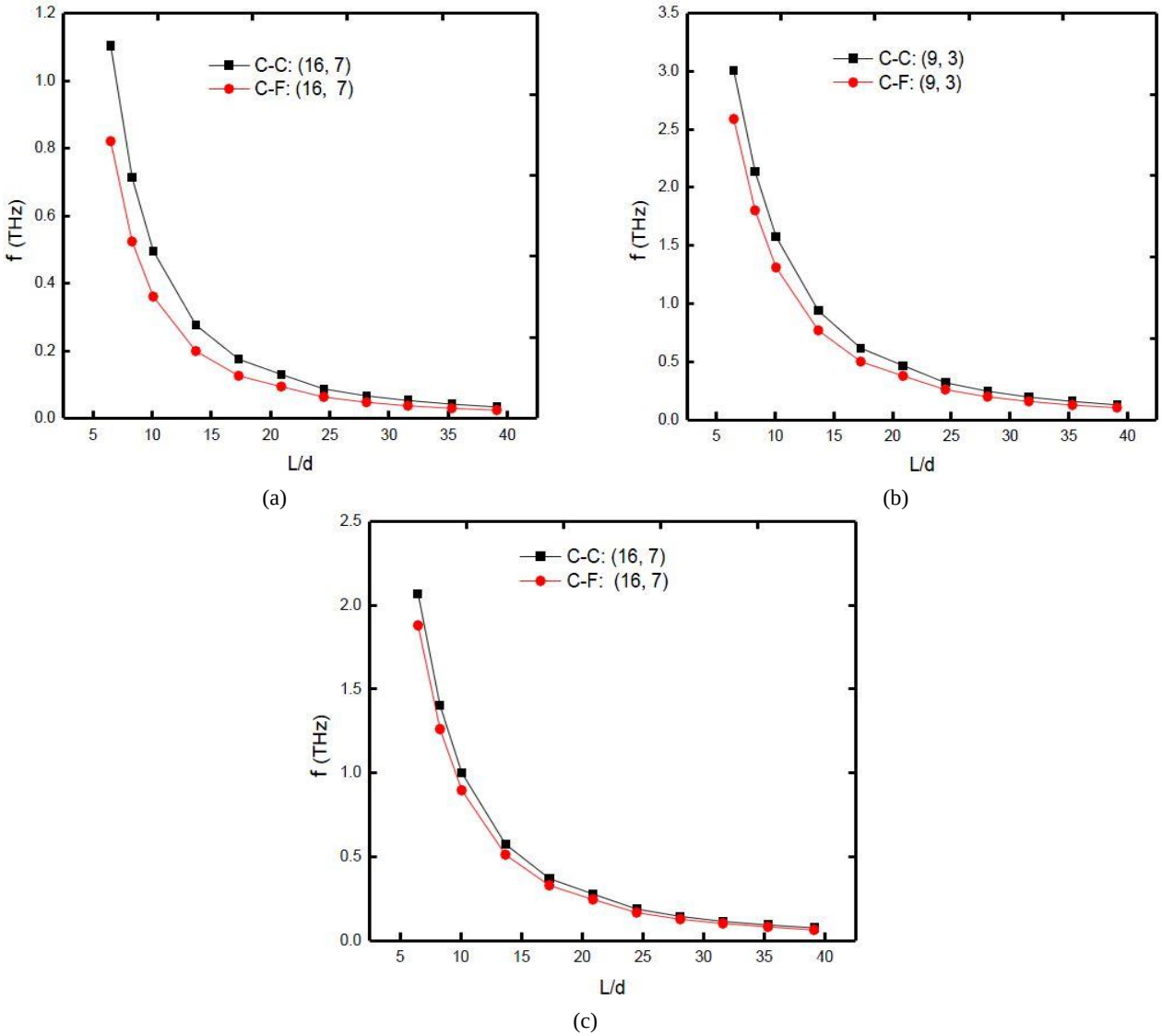

Fig. 14 Frequencies of chiral (6, 4), (9, 3), (16, 7) SWCNTs versus *L/d* with ρh = 820.80 nm

ORCID ID

Muzamal Hussain
http://orcid.org/0000-0002-6226-359X

References

Akgöz, B. and Civalek, Ö. (2012), "Investigation of size effects on static response of single-walled carbon nanotubes based on strain gradient elasticity", *Int. J. Computat. Methods*, **9**(2), 1240032. https://doi.org/10.1142/S0219876212400324

Ansari, R. and Rouhi, H. (2013), "Nonlocal Flügge shell model for vibrations of double-walled carbon nanotubes with different boundary conditions", *Int. J. Appl. Mech.*, **80**, 021006-1. https://doi.org/10.1142/S179329201250018X

Asghar, S., Hussain, M. and Naeem, M. (2019), "Non-local effect on the vibration analysis of double walled carbon nanotubes based on Donnell shell theory", *Physica E: Low-dimens. Syst. Nanostruct.*, **116**, 113726. https://doi.org/10.1016/j.physe.2019.113726

Asghar, S., Naeem, M.N., Hussain, M., Taj, M. and Tounsi, A. (2020), "Prediction and assessment of nolocal natural frequencies DWCNTs: Vibration analysis", *Comput. Concrete, Int. J.*, **25**(2), 133-144. https://doi.org/10.12989/cac.2020.25.2.133

Avcar, M. (2015), "Effects of rotary inertia shear deformation and non-homogeneity on frequencies of beam", *Struct. Eng. Mech., Int. J.*, **55**(4), 871-884. https://doi.org/10.12989/sem.2015.55.4.871

Avcar, M. (2019), "Free vibration of imperfect sigmoid and power law functionally graded beams", *Steel Compos. Struct., Int. J.*, **30**(6), 603-615. https://doi.org/10.12989/scs.2019.30.6.603

Azrar, A., Azrar, L. and Aljinaidi, A.A. (2011), "Length scale effect analysis on vibration behavior of single-walled Carbon Nanotubes with arbitrary boundary conditions", *Revue de Mécanique Appliqué et Théorique*, **2**, 475-485.

Chavan, S.G. and Lal, A. (2017), "Bending behavior of SWCNT reinforced composite plates", *Steel Compos. Struct., Int. J.*, **24**(5), 537-548. https://doi.org/10.12989/scs.2017.24.5.537

Civalek, Ö., Ersoy, H., Numanoğlu, H.M. and Akgöz, B. (2018), "Small size and rotary inertia effects on the natural frequencies of carbon nanotubes", *Curved Layer. Struct.*, **5**(1), 273-279. https://doi.org/10.1515/cls-2018-0020

Duan, W.H., Wang, C.M. and Zhang, Y.Y. (2007), "Calibration of nonlocal scaling effect parameter for free vibration of carbon

nanotubes by molecular dynamic", *J. Appl. Phys*., **10**1(2), 024305. https://doi.org/10.1063/1.2423140

Ebrahimi, F. and Habibi, S. (2017), "Low-velocity impact response of laminated FG-CNT reinforced composite plates in thermal environment", *Adv. Nano Res., Int. J.*, **5**(2), 69-97. https://doi.org/10.12989/anr.2017.5.2.069

Elishakoff, I. and Pentaras, D. (2009), "Fundamental natural frequencies of double-walled carbon nanotubes", *J. Sound Vib*., **322**, 652-664. https://doi.org/10.1016/j.jsv.2009.02.037

Emdadi, M., Mohammadimehr, M. and Navi, B.R. (2019), "Free vibration of an annular sandwich plate with CNTRC facesheets and FG porous cores using Ritz method", *Adv. Nano Res., Int. J*., **7**(2), 109-123. https://doi.org/10.12989/anr.2019.7.2.109

Fatahi-Vajari, A., Azimzadeh, Z. and Hussain, M. (2019), "Nonlinear coupled axial-torsional vibration of single-walled carbon nanotubes using Galerkin and Homotopy perturbation method", *Micro Nano Lett*., **14**(14), 1366-1371. https://doi.org/10.1049/mnl.2019.0203

Fazelzadeh, S.A. and Ghavanloo, E. (2012a), "Nonlocal anisotropic elastic shell model for vibrations of single-walled carbon nanotubes with arbitrary chirality", *Compos. Struct*., **94**(3), 1016-1022. https://doi.org/10.1016/j.compstruct.2011.10.014

Fereidoon, A., Rafiee, R. and Moghadam, R.M. (2013), "A modal analysis of carbon-nanotube-reinforced polymer by using a multiscale finite-element method", *Mech. Compos. Mater*., **49**(3), 325-332. https://doi.org/10.1007/s11029-013-9350-6

Flugge, S. (1973), *Stresses in Shells*, 2nd Edition, Springer, Berlin, Germany.

Gao, Y. and An, L. (2010), "A nonlocal elastic anisotropic shell model for microtubule buckling behaviors in cytoplasm", *Physica E*: *Low-dimens. Syst. Nanostruct*., **42**(9), 2406-2415. https://doi.org/10.1016/j.bbrc.2009.07.042

Ghavanloo, E. and Fazelzadeh, S.A. (2012b), "Vibration characteristics of single-walled carbon nanotubes based on an anisotropic elastic shell model including chirality effect", *Appl. Mathe. Model*., **36**(10), 4988-5000. https://doi.org/10.1016/j.apm.2011.12.036

Gibson, R.F., Ayorinde, E.O. and Wen, Y.F. (2007), "Vibrations of carbon nanotubes and their composites: a review", *Compos. Sci. Technol*., **67**(1), 1-28. https://doi.org/10.1016/j.compscitech.2006.03.031

Han, J., Globus, A., Jaffe, R. and Deardorff, G. (1997), "Molecular dynamics simulations of carbon nanotube-based gears", *Nanotechnology*, **8**(3), 95. https://doi.org/10.1088/0957-4484/8/3/001

Heydarpour, Y., Aghdam, M.M. and Malekzadeh, P. (2014), "Free vibration analysis of rotating functionally graded carbon nanotube-reinforced composite truncated conical shells", *Compos. Struct*., **117**, 187-200. http://doi.org/10.1016/j.compstruct.2014.06.023

Hussain, M. and Naeem, M.N. (2017), "Vibration analysis of single-walled carbon nanotubes using wave propagation approach", *Mech. Sci*., **8**(1), 155-164. https://doi.org/10.5194/ms-8-155-2017

Hussain, M. and Naeem, M. (2018a), "Vibration of single-walled carbon nanotubes based on Donnell shell theory using wave propagation approach", Chapter, Intechopen, *Novel Nanomaterials - Synthesis and Applications*. ISBN 978-953-51-5896-7 https://doi.org/10.5772/intechopen.73503

Hussain, M. and Naeem, M.N. (2018b), "Effect of various edge conditions on free vibration characteristics of rectangular plates", Chapter, Intechopen, *Advance Testing and Engineering*. ISBN 978-953-51-6706-8

Hussain, M. and Naeem, M. (2019a), "Vibration characteristics of single-walled carbon nanotubes based on non-local elasticity theory using wave propagation approach (WPA) including chirality", In: *Perspective of Carbon Nanotubes*.

Hussain, M. and Naeem, M.N. (2019b), "Effects of ring supports on vibration of armchair and zigzag FGM rotating carbon nanotubes using Galerkin's method", *Compos.*: *Part B. Eng.*, **163**, 548-561. https://doi.org/10.1016/j.compositesb.2018.12.144

Hussain, M. and Naeem, M. (2019c), "Rotating response on the vibrations of functionally graded zigzag and chiral single walled carbon nanotubes", *Appl. Mathe. Model*., **75**, 506-520. https://doi.org/10.1016/j.apm.2019.05.039

Hussain, M. and Naeem, M.N. (2020a), "Mass density effect on vibration of zigzag and chiral SWCNTs", *J. Sandw. Struct. Mater*. https://doi.org/10.1177/1099636220906257

Hussain, M. and Naeem, M.N. (2020b), "On mixing the Rayleigh-Ritz formulation with Hankel's function for vibration of fluid-filled Fluid-filled cylindrical shell", *J. Adv. Concrete Constr*., 1099636220906257. https://doi.org/10.1177/1099636220906257

Hussain, M., Naeem, M.N., Shahzad, A. and He, M. (2017), "Vibrational behavior of single-walled carbon nanotubes based on cylindrical shell model using wave propagation approach", *AIP Advances*, **7**(4), 045114. https://doi.org/10.1063/1.4979112

Hussain, M., Naeem, M., Shahzad, A. and He, M. (2018a), "Vibration characteristics of fluid-filled functionally graded cylindrical material with ring supports", Chapter, Intechopen, *Computational Fluid Dynamics*. ISBN 978-953-51-5706-9 https://doi.org/10.5772 /intechopen.72172

Hussain, M., Naeem, M.N., Shahzad, A., He, M.G. and Habib, S. (2018b), "Vibrations of rotating cylindrical shells with functionally graded material using wave propagation approach", *IMechE Part C*: *J. Mech. Eng. Sci*., **232**(23), 4342-4356. https://doi.org/10.1177/0954406218802320

Hussain, M., Naeem, M.N. and Isvandzibaei, M. (2018c), "Effect of Winkler and Pasternak elastic foundation on the vibration of rotating functionally graded material cylindrical shell", *Proceedings of the Institution of Mechanical Engineers*, *Part C*: *J. Mech. Eng. Sci*., **232**(24), 4564-4577. https://doi.org/10.1177/0954406217753459

Hussain, M., Naeem, M.N., Tounsi, A. and Taj, M. (2019a), "Nonlocal effect on the vibration of armchair and zigzag SWCNTs with bending rigidity", *Adv. Nano Res., Int. J*., **7**(6), 431-442. https://doi.org/10.12989/anr.2019.7.6.431

Hussain, M., Naeem, M.N. and Taj, M. (2019b), "Effect of length and thickness variations on the vibration of SWCNTs based on Flügge's shell model", *Micro Nano Lett*., **15**(1), 1-6. https://doi.org/10.1049/mnl.2019.0309

Hussain, M., Naeem, M.N. and Taj, M. (2019c), "Vibration characteristics of zigzag and chiral FGM rotating carbon nanotubes sandwich with ring supports", *J. Mech. Eng. Sci*., *Part C*, **233**(16), 5763-5780. https://doi.org/10.5772/intechopen.85948

Hussain, M., Naeem, M.N. and Tounsi, A. (2020a), "Simulating vibration of single-walled carbon nanotube based on Relagh-Ritz Method", *Adv. Nano Res., Int. J*., **8**(3), 221-234. https://doi.org/10.12989/anr.2020.8.3.221

Hussain, M., Naeem, M.N. and Tounsi, A. (2020b), "Numerical study for nonlocal vibration of orthotropic SWCNTs based on Kelvin's model", *Adv. Concrete Constr., Int. J*., **9**(3), 301-312. https://doi.org/10.12989/acc.2020.9.3.301

Jorio, A., Saito, R., Hafner, J.H., Lieber, C.M., Hunter, M., McClure, T., Dresselhaus, G. and Dresselhaus, M.S. (2001), "Structural (n,m) Determination of Isolated Single-Wall Carbon Nanotubes by Resonant Raman Scattering", *Phys. Rev. Lett*., **86**(6), 1118-1121. https://doi.org/10.1103/PhysRevLett.86.1118

Karami, B., Janghorban, M. and Tounsi, A. (2017), "Effects of triaxial magnetic field on the anisotropic nanoplates", *Steel Compos. Struct., Int. J.*, **25**(3), 361-374. https://doi.org/10.12989/scs.2017.25.3.361

Kotakoski, J., Krasheninnikov, A.V. and Nordlund, K. (2006), "Energetics, structure, and long-range interaction of vacancy-type defects in carbon nanotubes: Atomistic simulations", *Phys. Rev. B*, **74**, 245420/1-5. https://doi.org/10.12989/scs.2018.28.1.099

Kulathunga, D.D.T.K., Ang, K.K. and Reddy, J.N. (2009), "Accurate modeling of buckling of single-and double-walled carbon nanotubes based on shell theories", *J. Phys.: Condensed Matter*, **21**(43), 435301. https://doi.org/10.1088/0953-8984/21/43/435301

Madani, H., Hosseini, H. and Shokravi, M. (2016), "Differential cubature method for vibration analysis of embedded FG-CNT-reinforced piezoelectric cylindrical shells subjected to uniform and non-uniform temperature distributions", *Steel Compos. Struct., Int. J.*, **22**(4), 889-913. https://doi.org/10.12989/scs.2016.22.4.889

Mehar, K. and Panda, S.K. (2016a), "Geometrical nonlinear free vibration analysis of FG-CNT reinforced composite flat panel under uniform thermal field", *Compos. Struct.*, **143**, 336-346. https://doi.org/10.1016/j.compstruct.2016.02.038

Mehar, K. and Panda, S.K. (2016b), "Free vibration and bending behaviour of CNT reinforced composite plate using different shear deformation theory", *Proceedings of IOP Conference Series: Materials Science and Engineering*, **115**(1), 012014. https://doi.org/10.1088/1757-899X/115/1/012014

Mehar, K. and Panda, S.K. (2018a), "Dynamic response of functionally graded carbon nanotube reinforced sandwich plate", *Proceedings of IOP Conference Series: Materials Science and Engineering*, **338**(1), p. 012017. https://doi.org/10.1088/1757-899X/338/1/012017

Mehar, K. and Panda, S.K. (2018b), "Thermal free vibration behavior of FG-CNT reinforced sandwich curved panel using finite element method", *Polym. Compos.*, **39**(8), 2751-2764. https://doi.org/10.1002/pc.24266

Mehar, K. and Panda, S.K. (2018c), "Elastic bending and stress analysis of carbon nanotube-reinforced composite plate: Experimental, numerical, and simulation", *Adv. Polym. Technol.*, **37**(6), 1643-1657. https://doi.org/10.1002/adv.21821

Mehar, K. and Panda, S.K. (2018d), "Thermoelastic flexural analysis of FG-CNT doubly curved shell panel", *Aircr. Eng. Aerosp. Technol.*, **90**(1), 11-23. https://doi.org/10.1108/AEAT-11-2015-0237

Mehar, K. and Panda, S.K. (2018e), "Nonlinear finite element solutions of thermoelastic flexural strength and stress values of temperature dependent graded CNT-reinforced sandwich shallow shell structure", *Struct. Eng. Mech., Int. J.*, **67**(6), 565-578. https://doi.org/10.12989/sem.2018.67.6.565

Mehar, K. and Panda, S.K. (2019), "Multiscale modeling approach for thermal buckling analysis of nanocomposite curved structure", *Adv. Nano Res., Int. J.*, **7**(3), 181-190. https://doi.org/10.12989/anr.2019.7.3.181

Mehar, K., Panda, S.K., Dehengia, A. and Kar, V.R. (2016), "Vibration analysis of functionally graded carbon nanotube reinforced composite plate in thermal environment", *J. Sandw. Struct. Mater.*, **18**(2), 151-173. https://doi.org/10.1177/1099636215613324

Mehar, K., Panda, S.K. and Mahapatra, T.R. (2017a), "Thermoelastic nonlinear frequency analysis of CNT reinforced functionally graded sandwich structure", *Eur. J. Mech.-A/Solids*, **65**, 384-396. https://doi.org/10.1016/j.euromechsol.2017.05.005

Mehar, K., Panda, S.K., Bui, T.Q. and Mahapatra, T.R. (2017b), "Nonlinear thermoelastic frequency analysis of functionally graded CNT-reinforced single/doubly curved shallow shell panels by FEM", *J. Thermal Stress.*, **40**(7), 899-916. https://doi.org/10.1080/01495739.2017.1318689

Mehar, K., Panda, S.K. and Mahapatra, T.R. (2017c), "Theoretical and experimental investigation of vibration characteristic of carbon nanotube reinforced polymer composite structure", *Int. J. Mech. Sci.*, **133**, 319-329. https://doi.org/10.1016/j.ijmecsci.2017.08.057

Mehar, K., Panda, S.K. and Patle, B.K. (2017d), "Thermoelastic vibration and flexural behavior of FG-CNT reinforced composite curved panel", *Int. J. Appl. Mech.*, **9**(4), 1750046. https://doi.org/10.1142/S1758825117500466

Mehar, K., Mahapatra, T.R., Panda, S.K., Katariya, P.V. and Tompe, U.K. (2018a), "Finite-element solution to nonlocal elasticity and scale effect on frequency behavior of shear deformable nanoplate structure", *J. Eng. Mech.*, **144**(9), 04018094. https://doi.org/10.1061/(ASCE)EM.1943-7889.0001519

Mehar, K., Panda, S.K. and Mahapatra, T.R. (2018b), "Thermoelastic deflection responses of CNT reinforced sandwich shell structure using finite element method", *Scientia Iranica*, **25**(5), 2722-2737.

Mehar, K., Panda, S.K. and Patle, B.K. (2018c), "Stress, deflection, and frequency analysis of CNT reinforced graded sandwich plate under uniform and linear thermal environment: A finite element approach", *Polym. Compos.*, **39**(10), 3792-3809. https://doi.org/10.1002/pc.24409

Mehar, K., Panda, S.K. and Mahapatra, T.R. (2018d), "Nonlinear frequency responses of functionally graded carbon nanotube-reinforced sandwich curved panel under uniform temperature field", *Int. J. Appl. Mech.*, **10**(3), 1850028. https://doi.org/10.1142/S175882511850028X

Mehar, K., Panda, S.K., Devarajan, Y. and Choubey, G. (2019), "Numerical buckling analysis of graded CNT-reinforced composite sandwich shell structure under thermal loading", *Compos. Struct.*, **216**, 406-414. https://doi.org/10.1016/j.compstruct.2019.03.002

Moghadam, R.M., Hosseini, S.A. and Salehi, M. (2014), "The influence of Stone-Thrower-Wales defect on vibrational characteristics of single-walled carbon nanotubes incorporating Timoshenko beam element", *Physica E: Low-dimens. Syst. Nanostruct.res*, **62**, 80-89. https://doi.org/10.1016/j.physe.2014.04.008

Mohammadimehr, M. and Alimirzaei, S. (2016), "Nonlinear static and vibration analysis of Euler-Bernoulli composite beam model reinforced by FG-SWCNT with initial geometrical imperfection using FEM", *Struct. Eng. Mech., Int. J.*, **59**(3), 431-454. https://doi.org/10.12989/sem.2016.59.3.431

Natsuki, T., Endo, M. and Tsuda, H. (2006), "Vibration analysis of embedded carbon nanotubes using wave propagation approach", *J. Appl. Phys.*, **99**(3), 034311. https://doi.org/10.1063/1.2170418

Paliwal, D.N., Kanagasabapathy, H. and Gupta, K.M. (1995), "The large deflection of an orthotropic cylindrical shell on a Pasternak foundation", *Compos. Struct.*, **31**(1), 31-37. https://doi.org/10.1016/0263-8223(94)00068-9

Rafiee, R. and Moghadam, R.M. (2012), "Simulation of impact and post-impact behavior of carbon nanotube reinforced polymer using multi-scale finite element modeling", *Computat. Mater. Sci.*, **63**, 261-268. https://doi.org/10.1016/j.commatsci.2012.06.010

Rouhi, H., Ansari, R. and Arash, B. (2013), "Vibrational analysis of double-walled carbon nanotubes based on the nonlocal Donnell shell theory via a new numerical approach", *Iran J. Sci Technol. Transact. B-Eng.*, **37**, 91-105.

Selim, M.M. (2010), "Torsional vibration of carbon nanotubes under initial compression stress", *Brazil. J. Phys.*, **40**(3), 283-287. http://dx.doi.org/10.1590/S0103-97332010000300004

Semmah, A., Heireche, H., Bousahla, A.A. and Toumsi, A. (2019), "Thermal buckling analysis of SWBNNT on Winkler foundation by nonlocal FSDT", *Adv. Nano Res., Int. J.*, **7**(2), 89-98. https://doi.org/10.12989/anr.2019.7.2.089

Sharma, P., Singh, R. and Hussain, M. (2019), "On modal analysis

of axially functionally graded material beam under hygrothermal effect", *Proceedings of the Institution of Mechanical Engineers, Part C: J. Mech. Eng. Sci.*, **234**(5), 1085-1101. https://doi.org/10.1177/0954406219888234

Sofiyev, A.H. and Avcar, M. (2010), "The stability of cylindrical shells containing an FGM layer subjected to axial load on the Pasternak foundation", *Engineering*, **2**(4), 228-236. https://doi.org/10.4236/eng.2010.24033

Swaddiwudhipong, S., Tian, J. and Wang, C.M. (1995), "Vibrations of cylindrical shells with intermediate supports", *J. Sound Vib.*, **187**, 69-93. https://doi.org/10.1006/jsvi.1995.0503

Taj, M., Safeer, M., Hussain, M., Naeem, M.N., Ahmad, M., Abbas, K., Khan, A.Q. and Tounsi, A. (2020), "Effect of external force on buckling of cytoskeleton intermediate filaments within viscoelastic media", *Comput. Concrete, Int. J.*, **25**(3), 205-214. https://doi.org/10.12989/cac.2020.25.3.205

Tohidi, H., Hosseini-Hashemi, S.H. and Maghsoudpour, A. (2018), "Size-dependent forced vibration response of embedded micro cylindrical shells reinforced with agglomerated CNTs using strain gradient theory", *Smart Struct. Syst., Int. J.*, **22**(5), 527-546. https://doi.org/10.12989/sss.2018.22.5.527

Usuki, T. and Yogo, K. (2009), "Beam equations for multi-walled carbon nanotubes derived from Flugge shell theory", *Proceedings of Royal Society A*, **465**(2104). https://doi.org/10.1098/rspa.2008.0394

Wang, J. and Gao, Y. (2016), "Nonlocal orthotropic shell model applied on wave propagation in microtubules", *Appl. Mathe. Model.*, **40**(11-12), 5731-5744. https://doi.org/10.1016/j.apm.2016.01.013

Wang, V. and Liew, K.M. (2007), "Application of nonlocal continuum mechanics to static analysis of micro-and nano-structures", *Phys. Lett. A*, **363**, 236-242. http://dx.doi.org/10.1016/j.physleta.2006.10.093

Zhang, Y.Y., Wang, C.M. and Tan, V.B.C. (2009), "Assessment of Timoshenko beam models for vibrational behavior of single-walled carbon nanotubes using molecular dynamics", *Adv. Appl. Math. Mech.*, **1**, 89-106.

Zou, R.D. and Foster, C.G. (1995), "Simple solution for buckling of orthotropic circular cylindrical shells", *Thin-Wall. Struct.*, **22**(3), 143-158. https://doi.org/10.1016/0263-8231(94)00026-V

CC